JVI Journals.ASM.org

A Second CRM1-Dependent Nuclear Export Signal in the Influenza A Virus NS2 Protein Contributes to the Nuclear Export of Viral Ribonucleoproteins

Shengping Huang,[a,d] Jingjing Chen,[a,d] Quanjiao Chen,[a] Huadong Wang,[a,d] Yanfeng Yao,[a,d] Jianjun Chen,[a] Ze Chen[a,b,c]

State Key Laboratory of Virology, Wuhan Institute of Virology, Chinese Academy of Sciences, Wuhan, China[a]; College of Life Sciences, Hunan Normal University, Changsha, Hunan, China[b]; Shanghai Institute of Biological Products, Shanghai, China[c]; Graduate University of Chinese Academy of Sciences, Beijing, China[d]

Influenza A virus NS2 protein, also called nuclear export protein (NEP), is crucial for the nuclear export of viral ribonucleoproteins. However, the molecular mechanisms of NEP mediation in this process remain incompletely understood. A leucine-rich nuclear export signal (NES2) in NEP, located at the predicted N2 helix of the N-terminal domain, was identified in the present study. NES2 was demonstrated to be a transferable NES, with its nuclear export activity depending on the nuclear export receptor chromosome region maintenance 1 (CRM1)-mediated pathway. The interaction between NEP and CRM1 is coordinately regulated by both the previously reported NES (NES1) and now the new NES2. Deletion of the NES1 enhances the interaction between NEP and CRM1, and deletion of the NES1 and NES2 motifs completely abolishes this interaction. Moreover, NES2 interacts with CRM1 in the mammalian two-hybrid system. Mutant viruses containing NES2 alterations generated by reversed genetics exhibit reduced viral growth and delay in the nuclear export of viral ribonucleoproteins (vRNPs). The NES2 motif is highly conserved in the influenza A and B viruses. The results demonstrate that leucine-rich NES2 is involved in the nuclear export of vRNPs and contributes to the understanding of nucleocytoplasmic transport of influenza virus vRNPs.

The transport of macromolecules between the nucleus and the cytoplasm is mediated by nuclear pore complexes (NPCs) embedded in the nuclear envelope. Small molecules can pass through NPCs via passive diffusion, whereas the translocation of larger molecules (>50 kDa) generally requires specific transport receptors (1). Exportins are a group of transport receptors responsible for the nuclear export of cargo molecules. Chromosome region maintenance 1 (CRM1; also called exportin1/Xpo1) has been identified as an export factor for the leucine-rich nuclear export signal (NES) and plays an important role in the nuclear export of leucine-rich NES-containing proteins (2–4). Cellular CRM1-mediated nuclear export can be specifically inhibited by the nuclear export inhibitor leptomycin B (LMB) (5, 6).

The genome of influenza A virus contains eight single-stranded RNA segments packed into viral ribonucleoprotein (vRNP) complexes (7). Unlike most RNA viruses replicated in the cytoplasm, influenza virus is rare in that it replicates in the nucleus. The newly synthesized progeny vRNP complex, which consists of the negative-strand viral RNA (vRNA), the trimeric polymerase complex of PB1-PB2-PA, and the nucleoprotein (NP) in the nucleus, requires export to the assembly site in the cytoplasm for envelopment and budding during the late stage of infection (8, 9). Both M1 and NS2 proteins are involved in the nuclear export of vRNPs (10, 11). NS2 protein was renamed "nuclear export protein" (NEP) because it has been confirmed to feature in purified virus particles and to function as a nuclear export protein for vRNPs (11–14).

Segment 8 of influenza A virus encodes two proteins, namely, NS1 and NEP, via differential splicing (15). Full-length NEP consists of 121 amino acids (aa), with the N-terminal domain comprising amino acids 1 to 53 and the C-terminal domain consisting of amino acids 54 to 121 (16). The N-terminal domain of NEP contains leucine-rich NES1 (12-ILMRMSKMQL-21) located at amino acids 12 to 21, which can functionally replace the NES of human immunodeficiency virus type 1 Rev protein. In addition to its role in the regulation of transcription and replication of the influenza virus RNA genome (17), NEP is crucial for the nuclear export of vRNPs (11). The vRNP nuclear export capability of a mutant virus with altered NES1 is delayed compared with that of the wild-type virus (18). Furthermore, influenza virus M1 protein functions as a bridge between NEP and vRNP by binding to the C-terminal portion of NEP (16, 19). Elton et al. suggested that NP, not NEP and M1 proteins, is responsible for the nuclear export of vRNPs and showed that cellular localization of NEP in transfected cells is not affected by LMB treatment (20). However, several studies have also demonstrated that NEP accumulates in the nucleus in the presence of LMB (21–23). In addition, biochemical assays show that NEP associates with the export factor hCRM1 and several nucleoporins (11, 24). LMB treatment specifically inhibits the nuclear export of vRNPs (18, 23), demonstrating that the nuclear export of vRNPs is mediated by NEP in an hCRM1-dependent manner. It was therefore suggested that vRNPs exist as hCRM1-NEP-M1-vRNP complexes in the nucleus, are exported to the cytoplasm, and subsequently are incorporated into the progeny virions (8, 16, 25). Alterations in NES abolish interactions between leucine-rich NES-containing proteins and the CRM1 receptor. Neumann et al. showed that deletion of the published NES of NEP results in much stronger interactions with hCRM1 com-

Received 10 October 2011 **Accepted** 22 October 2012
Published ahead of print 31 October 2012
Address correspondence to Ze Chen, chenze2005@hotmail.com.
Supplemental material for this article may be found at http://dx.doi.org/10.1128/JVI.06519-11.

doi:10.1128/JVI.06519-11

pared with that by full-length NEP, suggesting that NEP mediates the nuclear export of influenza virus vRNPs through NEP interaction with hCRM1 in an NES-independent manner (26).

The mechanism by which NEP mediates the nuclear export of vRNPs requires further elucidation. In the present study, the experimental data suggest the existence of a hitherto unsuspected NES in influenza A virus NEP. The previously reported NES, which contains amino acids 12 to 21 of NEP (11, 18), is called NES1, and the newly identified NES is named NES2. NES2 is a transferable, leucine-rich, and CRM1-dependent NES. We demonstrate that NES2 is involved in the nuclear export of vRNPs and propagation of influenza virus. The results of the present research provide novel insights into the function of NEP and further elucidate the molecular mechanism underlying the nuclear export of influenza virus vRNPs.

MATERIALS AND METHODS

Cells and viruses. 293T and HeLa cells were cultured in Dulbecco's modified Eagle's medium (DMEM; Gibco) supplemented with 10% fetal bovine serum (FBS; Gibco). MDCK cells were cultured in minimum essential medium (MEM; Gibco) containing 10% FBS. The influenza virus A/Puerto Rico/8/1934 (H1N1) and A/chicken/Helan/12/2004 (H5N1) strains were preserved in our laboratory (27, 28).

Plasmid construction. The open reading frame (ORF) of NEP of the influenza virus A/chicken/Helan/12/2004 (H5N1) strain was cloned into the EcoRI-SalI sites of the enhanced green fluorescent protein (EGFP)-tagged plasmid pEGFP-C1 (Clontech) by PCR for fluorescent confocal microscopy. Truncated mutants corresponding to the amino acid mutations designated in $NEP_{\Delta NES1}$, $NEP_{\Delta NES1^{1-96}}$, $NEP_{\Delta NES1^{1-81}}$, $NEP_{\Delta NES1^{1-60}}$, $NEP_{\Delta NES1^{1-45}}$, NEP^{22-121}, NEP^{46-121}, and NEP^{61-121}, or the point mutants corresponding to NEP(M31A), NEP(F35A), NEP(L38A), NEP(L40A), and NEP(L38A/L40A) were constructed via PCR using the plasmid pEGFP-NEP as a template with corresponding primers. Plasmids pEGFP-NEP(28–45)-EGFP, pEGFP-NEP(28–40)-EGFP, pEGFP-NEP(31–45)-EGFP, and pEGFP-NEP(31–40)-EGFP were constructed in two steps. First, the corresponding sequence of NEP was fused to the N-terminal region of the EGFP ORF via PCR. Second, the fused PCR products were cloned into the expression vector pEGFP-C1 via standard enzyme digestion and ligation manipulation. The ORF of NEP was cloned into the SalI-EcoRV sites of the expression vector pBIND (Promega) via PCR for mammalian two-hybrid assays. Various NEP truncation mutants or point mutations used for the interaction assays were generated via PCR and cloned into the same sites of the pBIND vector. The ORF of hCRM1 was amplified from the plasmid pSG5-CRM1-GFP (from Maarten Fornerod, NCI, Amsterdam, The Netherlands), and the product of the hCRM1 ORF was cloned into the expression vector pACT (Promega). Eight gene fragments were digested with BsmBI and cloned into the BsmBI sites of the expression vector pHW2000 to construct eight plasmids for reverse genetics (29). Recombinant plasmids carrying different influenza virus A/Puerto Rico/8/1934 (H1N1) gene segments were named pHW-PR8-PB2, pHW-PR8-PB1, pHW-PR8-PA, pHW-PR8-HA, pHW-PR8-NP, pHW-PR8-NA, pHW-PR8-M, and pHW-PR8-NS. The NS fragment was amplified and cloned into the pGEM-T vector (Promega) for site-directed mutagenesis to generate NEP NES2 mutant virus. The NS mutant was then subcloned into vector pHW2000 for reverse genetics manipulations. All constructs were sequenced in full.

Site-directed mutagenesis. Site-directed mutagenesis was performed using the QuickChange site-directed mutagenesis kit (Stratagene) following the instructions of the manufacturer. All point mutations were verified via DNA sequencing.

Cell culture and transfection. 293T, MDCK, and HeLa cells were maintained in a 37°C humidified atmosphere containing 5% CO_2. Cells for transfection were seeded on dishes. After overnight growth, the cells became 70% confluent and were transfected with the corresponding plasmids using the transfection reagent Lipofectamine 2000 (Invitrogen) in a nonserum medium according to the instructions of the manufacturer. After 5 h of incubation, the medium was replaced with a completely fresh medium.

Western blot analysis. 293T cells were plated into six-well plates and transfected transiently with the indicated plasmids after 24 h. Twenty-four hours after transfection, the cells were harvested, washed twice with cold phosphate-buffered saline (PBS), and lysed with a cell lysis buffer (Cell Signaling). Cell lysates were fractionated using SDS-PAGE, blotted onto polyvinylidene difluoride (PVDF) membranes, and then immunoblotted with primary antibodies. Afterwards, blots were developed using horseradish peroxidase (HRP)- or alkaline phosphatase (AP)-conjugated secondary antibodies. Finally, staining was performed using the Super-Signal West Pico chemiluminescent substrate (Pierce) or substrate solutions (75 mg/ml nitro blue tetrazolium [NBT], 50 mg/ml 5-bromo-4-chloro-3-indolyl phosphate [BCIP], 0.1 M NaCl, 0.05 M $MgCl_2$, 0.1 M Tris-HCl [pH 9.5]).

Mammalian two-hybrid assay. 293T cells were cotransfected with 300 ng of the pBIND fusion construct, 300 ng of the pACT fusion construct, and 300 ng of the reporter gene construct pG5*luc* (Promega) per well in a 24-well plate using Lipofectamine 2000 to analyze the interaction of NEP or its mutants with hCRM1 in mammalian cells. The cells were then harvested, washed twice with cold PBS, and lysed with passive lysis buffer (Promega) 48 h after transfection. A luciferase assay was performed using a dual-luciferase reporter assay system (Promega) according to the specifications of the manufacturer. *Renilla* luciferase activity was used to correct for the variation in transfection efficiency. After sequential quantification of firefly and *Renilla* luciferase activities in the cell lysates, the binding interaction between the two proteins was calculated as a firefly/*Renilla* luciferase activity ratio to obtain relative activity. Experiments were performed in triplicate, and luciferase activity was determined using a T20/20 luminometer (Turner Designs, Sunnyvale, CA).

Fluorescence microscopy. 293T, MDCK, HeLa, or COS-7 cells were seeded on glass coverslips and transfected with the EGFP-tagged fusion constructs to yield cells expressing the EGFP-tagged fusion proteins. Twenty-four hours after transfection, the cells were washed with PBS, fixed with 4% paraformaldehyde (pH 7.4) for 20 min, permeabilized with 0.2% Triton X-100 in PBS for 15 min, and then stained with the bisbenzimidazole derivative Hoechst 33258 for 10 min. LMB was then added to the desired wells 21 h posttransfection at a final concentration of 11 nM for 3 h. Hoechst 33258 and LMB were both purchased from Sigma (St. Louis, MO). For the indirect immunofluorescence assay, MDCK cells were infected with the wild-type virus or the indicated mutant virus at a multiplicity of infection (MOI) of 1. At 5 h or 7 h postinfection, MDCK cells were fixed in 4% paraformaldehyde, permeabilized with 0.5% Triton X-100, blocked with 5% nonfat milk, and stained with mouse anti-NP antibodies, followed by incubation with a fluorescein isothiocyanate (FITC)-conjugated anti-mouse IgG (Millipore). Fluorescence image analysis was performed on a Leica laser-scanning confocal microscope with the associated software, as previously described (30).

Viral RNA extraction, reverse transcription, PCR, DNA sequencing, and real-time PCR. Viruses were inoculated into 10-day-old chicken embryos. The allantoic fluid was collected after 48 h, and viral RNA was extracted by lysing of the viruses with TRIzol LS reagent (Life Technologies, Inc.). The RNA was reverse transcribed into single-stranded DNA using Moloney murine leukemia virus (MMLV) reverse transcriptase (New England BioLabs). All segments were amplified with the Phusion high-fidelity PCR kit (New England BioLabs), using segment-specific primers as previously described (31). PCR products were purified using the Cycle-pure and gel extraction kits (Omega Bio-Tek), and fragments were cloned into the pGEM-T Easy vector. Fragments were sequenced via the dideoxy method using a 3730 DNA sequencer (Applied Biosystems), and sequencing reactions were performed according to the instructions of the manufacturer. The real-time PCR assay for the detection of vRNA copies was performed as described previously (32).

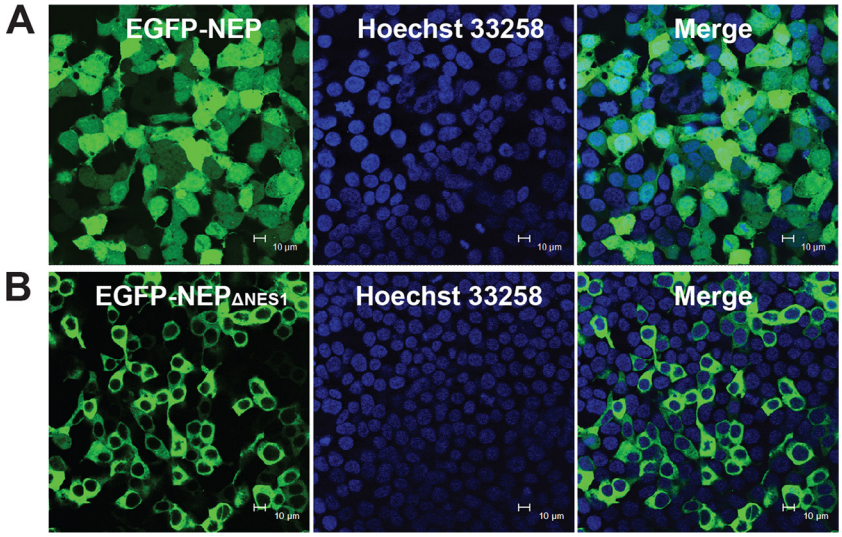

FIG 1 Subcellular localization of transiently expressed influenza virus A/chicken/Helan/12/2004 (H5N1) NEP and its deletion mutant, $NEP_{\Delta NES1}$, in 293T cells. (A) EGFP-NEP expressed in 293T cells. (B) EGFP-$NEP_{\Delta NES1}$ expressed in 293T cells. Cells were examined via fluorescence microscopy 24 h posttransfection. EGFP-NEP and EGFP-$NEP_{\Delta NES1}$ fluorescence is green. Cell nuclei are pseudocolored blue, following staining with Hoechst 33258 dye. Bars, 10 μm.

Generation of recombinant virus from cloned cDNA. Generation of recombinant virus based on the eight-plasmid system was carried out as previously described (29). Briefly, 1 μg of each plasmid (pHW-PR8-PB2, pHW-PR8-PB1, pHW-PR8-PA, pHW-PR8-HA, pHW-PR8-NP, pHW-PR8-NA, pHW-PR8-M, pHW-PR8-NS, or the NS mutant) was combined with 16 μl Lipofectamine 2000 (2 μl per μg DNA) (Invitrogen), and the mixture was incubated at room temperature for 30 min and then transferred to monolayers of 10^6 293T cells on six-well plates. After 6 h, the mixture was removed from the cells and replaced with Opti-MEM (Gibco-BRL) containing 5% fetal calf serum. Seventy-two hours after transfection, the culture medium was collected and inoculated onto 10-day-old specific-pathogen-free (SPF) chicken embryos for virus propagation.

Replicative properties of the rescued viruses. Growth curves were used to analyze the replication properties of the rescued viruses. MDCK cells were inoculated with the indicated virus at an MOI of 0.01. Virus suspensions were removed, and 3 ml of MEM containing 2.0 μg/ml trypsin was added to them after incubation at 37°C for 1 h. Culture media were collected every 12 h for 60 h after infection. The viral titer of each sampling, expressed as 50% tissue culture infective dose ($TCID_{50}$), was calculated using the Reed-Muench method (33).

RESULTS

Subcellular localization of influenza A virus NEP and its NES1-deleted mutant in 293T cells. NEP of influenza virus A/chicken/Helan/12/2004 (H5N1) contains the leucine-rich NES1 motif, which consists of amino acids 12 to 21 in its N-terminal region. To determine whether or not NES1 regulates the subcellular localization of NEP, two enhanced green fluorescent protein (EGFP)-tagged plasmids, pEGFP-NEP and pEGFP-$NEP_{\Delta NES1}$, were constructed to express the full-length and NES1-deleted versions of NEP, respectively. 293T cells were transfected with plasmids encoding EGFP-NEP and EGFP-$NEP_{\Delta NES1}$. Subcellular localization of expressed EGFP-tagged fusion proteins was detected using fluorescence microscopy 24 h posttransfection. Figure 1A shows that full-length NEP was distributed throughout the cytoplasm and nucleus. This pattern of distribution is in accordance with that of NEP in the previous report (34). Unexpectedly, the NES1-deficient construct EGFP-$NEP_{\Delta NES1}$ was localized exclusively in the cytoplasm (Fig. 1B), suggesting that another previously undiscovered NES that is sufficient to induce the cytoplasmic accumulation of the NES1-deleted mutant exists in $NEP_{\Delta NES1}$.

Mediation of the nuclear export of the $NEP_{\Delta NES1}$ via a CRM1-dependent pathway. LMB is a potent and highly specific nuclear export inhibitor that alkylates and inactivates the cellular export factor CRM1. The effects of LMB on the nuclear export of EGFP-$NEP_{\Delta NES1}$ in different cell lines were investigated. MDCK and HeLa cells were transiently transfected with pEGFP-$NEP_{\Delta NES1}$ and then treated (or not treated) with 11 nM LMB for 3 h and analyzed via fluorescence microscopy at 21 h posttransfection,. Cellular distributions of EGFP-$NEP_{\Delta NES1}$ were exclusively located in the cytoplasm in the absence of LMB (−LMB) (Fig. 2A and B). In contrast, LMB treatment blocked nuclear exports of EGFP-$NEP_{\Delta NES1}$ and nuclear retention was observed in both cell lines (+LMB) (Fig. 2A and B). As a negative control, cellular localization of the non-fusion protein EGFP was distributed in both the cytoplasm and nucleus regardless of LMB treatment (Fig. 2C). These results suggest the existence of a putative CRM1-dependent NES in $NEP_{\Delta NES1}$.

Cytoplasmic distribution of $NEP_{\Delta NES1}$. To identify sequence elements within $NEP_{\Delta NES1}$ that are responsible for its nuclear export, a series of EGFP-fused $NEP_{\Delta NES1}$ truncation mutants was constructed, as depicted in Fig. 3A. First, Western blot analysis of transfected cell lysates was performed using anti-EGFP antibodies to confirm the expression of truncation mutants of $NEP_{\Delta NES1}$. All constructs were correctly expressed and largely in line with their expected molecular weights (Fig. 3B). HeLa cells were then transfected with the constructs described above, and distributions of EGFP-$NEP_{\Delta NES1}$ truncation proteins were analyzed via fluorescence microscopy. Figure 3C showed that progressive truncation mutants from the C terminus up to amino acid 45 had no effect on the subcellular localization of EGFP-$NEP_{\Delta NES1}$ fusion proteins. All EGFP-tagged truncation mutants, including those containing amino acids 1 to 96, 1 to 81, 1 to 60, and 1 to 45, were localized exclusively in the cytoplasm in the absence of LMB. Truncations

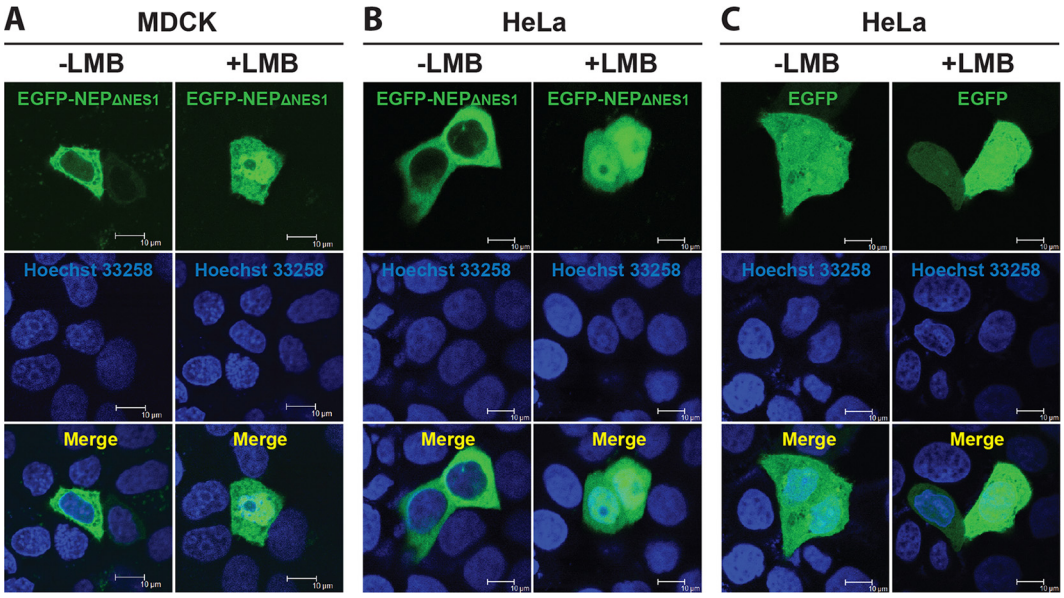

FIG 2 Cytoplasmic localization of EGFP-NEP$_{\Delta NES1}$ is sensitive to the nuclear export inhibitor LMB. (A) Cytoplasmic localization of EGFP-NEP$_{\Delta NES1}$ is inhibited following treatment with LMB in MDCK cells. (B) Cytoplasmic localization of EGFP-NEP$_{\Delta NES1}$ in HeLa cells is inhibited following treatment with LMB. (C) Subcellular localization of the negative control EGFP is not sensitive to LMB. MDCK or HeLa cells were transiently transfected with the EGFP-NEP$_{\Delta NES1}$ plasmid or the control vector pEGFP-C1 and treated (+LMB) or not treated (−LMB) with 11 nM LMB for 3 h at 21 h posttransfection. Cells were then fixed, permeabilized, and stained with Hoechst 33258 dye. Bars, 10 μm.

rapidly accumulated in the nucleus after LMB treatment, suggesting that putative NES was located within the 45 N-terminal amino acids. Further truncation up to amino acid 11 drastically changed the subcellular localization, and the resultant truncated protein, EGFP-NEP$_{\Delta NES1}$(1–11), was distributed in both the cytoplasm and nucleus. Moreover, three mutants with truncations from the N terminus, namely, EGFP-NEP$_{\Delta NES1}$(22–121), EGFP-NEP$_{\Delta NES1}$(46–121), and EGFP-NEP$_{\Delta NES1}$(61–121), were generated. EGFP-NEP$_{\Delta NES1}$(22–121) was exclusively distributed in the cytoplasm and showed sensitivity to LMB treatment, whereas EGFP-NEP$_{\Delta NES1}$(46–121) and EGFP-NEP$_{\Delta NES1}$(61–121) were localized in both the cytoplasm and nucleus and showed insensitivity to LMB treatment. These data indicate that the region between amino acids 22 and 45 is crucial for the cytoplasmic localization of NEP$_{\Delta NES1}$ and possibly contains an NES.

Identification of a functional NES in the predicted helix N2 region of influenza A virus NEP. The region between amino acids 22 and 45 contributes to the nuclear export of NEP$_{\Delta NES1}$; thus, the NES sequence in this region was further refined. Various deletion mutants in this region were fused with two tandem EGFP molecules (Fig. 4A), and the subcellular localization of these fusion proteins was examined. Two tandem EGFPs were found in both the nucleus and cytoplasm and were insensitive to LMB treatment. Cells transfected with pEGFP-(28–45)-EGFP, pEGFP-(28–40)-EGFP, pEGFP-(31–45)-EGFP, pEGFP-(31–40)-EGFP, and fusion proteins showed complete cytoplasmic localization and rapidly accumulated in the nucleus after LMB treatment (Fig. 4A). In addition, the $_{31}$MITQFESLKL$_{40}$ sequence revealed a stretch of hydrophobic amino acids that completely matched an NES consensus ($\Phi X_{2-3}\Phi X_2\Phi X\Phi$, where "Φ" represents any hydrophobic amino acid, such as leucine, isoleucine, valine, tryptophan, or methionine, and "X" represents any amino acid) (Fig. 4B). Collectively, these results suggest that 31-MITQFESLKL-40 amino acid residues form a functional, transferable, and CRM1-dependent NES (NES2). NEP of influenza virus A/chicken/Helan/12/2004 (H5N1) contains two predicted helix regions in its N-terminal domain, called helices N1 and N2 (16). The previously published NES1 motif is located in the predicted helix N1 region, whereas the NES2 motif reported in the present study is located in the predicted helix N2 region.

To determine the contributions of the hydrophobic residues within NES2 to its nuclear export activity, alanine-scanning mutagenesis of the hydrophobic residues within NES2 was performed and the cellular localization of these NES2 mutants fused with two tandem EGFPs was observed. The classic Rev NES motif was used as the positive control, whereas the M10 mutant (R-M10) of the Rev NES motif was used as the negative control (22). Rev NES is sufficient to induce cytoplasmic localization of the two tandem EGFPs in the positive control. In contrast, the M10 mutant of the Rev NES motif eliminated the cytoplasmic distribution of EGFP fusion proteins in the negative control (Fig. 4C). Both influenza A virus NES1 and NES2 mediated the cytoplasmic localization of EGFP fusion proteins. The cytoplasmic distribution of the fusion protein EGFP-NES2-EGFP was remarkably disrupted when residues aligned with high-consensus sites (M31, F35, L38, and L40) were replaced with alanine. In addition, double-point mutation NEP(L38A/L40A) resulted in nuclear retention of the mutant protein. The isoleucine at position 32 was not critical to cytoplasmic distribution; cytoplasmic distribution still occurred when isoleucine was replaced with alanine (Fig. 4C). These data indicate that hydrophobic residues on the highly conserved sites, specifically, M31, F35, L38, and L40, are crucial for the nuclear export activity of NES2.

Five EGFP-tagged plasmids, namely, pEGFP-NEP(M31A), pEGFP-(F35A), pEGFP-NEP(L38A), pEGFP(L40A), and pEGFP (L38A/L40A), were constructed for serial NEP mutation expres-

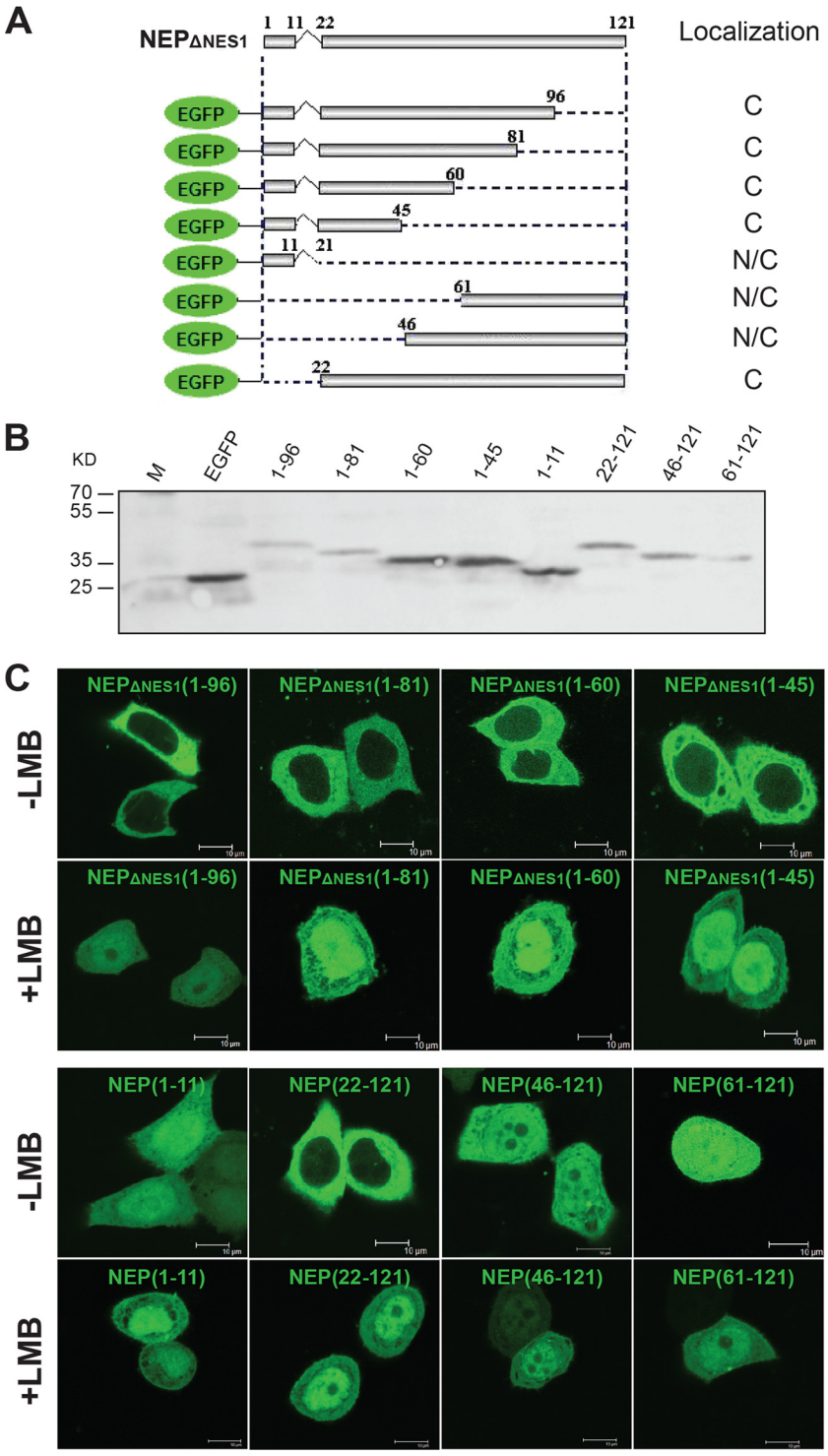

FIG 3 Mapping of subcellular localization signals of the influenza virus A/chicken/Helan/12/2004 (H5N1) $NEP_{\Delta NES1}$. (A) Schematic illustration of influenza A virus $NEP_{\Delta NES1}$ and its truncated derivatives. HeLa cells were transfected with EGFP-$NEP_{\Delta NES1}$ fusion constructs. About 24 h posttransfection, GFP was visualized via confocal microscopy. Subcellular localizations of the EGFP-$NEP_{\Delta NES1}$ mutants are summarized on the right. C, predominantly cytoplasmic localization; N/C, both nuclear and cytoplasmic localization. (B) Truncated derivatives of EGFP-$NEP_{\Delta NES1}$ fusion proteins identified via Western blotting of transiently transfected HEK293T cells. Cell lysates of HEK293T cells transfected with the EGFP-$NEP_{\Delta NES1}$ truncated constructions were analyzed via Western blotting with anti-GFP polyclonal antibodies. The sizes of the molecular mass (M_r) standards are shown on the left. (C) Subcellular distribution of EGFP-$NEP_{\Delta NES1}$ truncated constructions in transfected HeLa cells in the absence (−LMB) or presence (+LMB) of LMB. HeLa cells were transfected with the truncated constructions. About 21 h posttransfection, the cells were treated with or without 11 nM LMB for 3 h prior to fluorescence imaging using a 100× oil immersion objective lens. Bars, 10 μm.

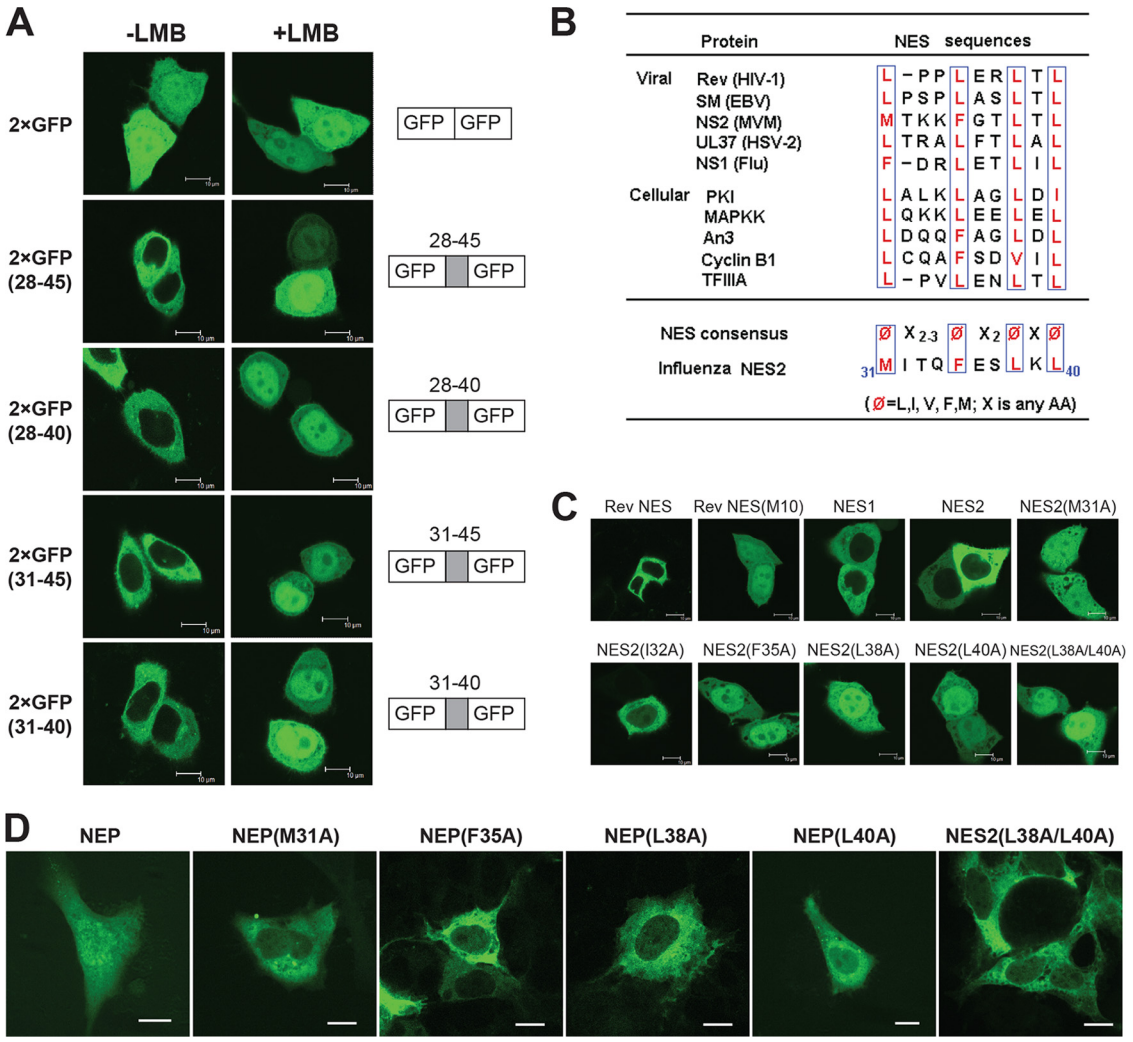

FIG 4 Identification of a functional and transferable leucine-rich NES in the influenza virus A/chicken/Helan/12/2004 (H5N1) NEP. (A) Mapping regions in amino acid sequence positions 22 to 45 of the influenza A virus NEP can mediate the nuclear export of two tandem EGFPs. Influenza A virus NEP fragments according to amino acid sequences 28 to 45, 28 to 40, 31 to 45, and 31 to 40 were inserted in frame between two EGFPs. These constructs were transfected into HeLa cells. About 21 h after transfection, cells were treated with (+LMB) or without (−LMB) 11 nM LMB for 3 h. GFP was then visualized via confocal microscopy. The schematic illustration of these constructs and their representative images are shown. (B) Amino acid residues 31 to 40 of influenza A virus NEP containing a leucine-rich motif are aligned with leucine-rich HIV-1 Rev-like NES consensus sequences of previously characterized cellular proteins and viral proteins. Conserved hydrophobic residues are shown in red. In the NES consensus sequence, "X" represents any amino acid and "Φ" represents any hydrophobic residue. (C) Fusion of the Rev NES sequence or influenza A virus NEP NES1 (aa 12 to 23) or NES2 (aa 31 to 40) to EGFP causes localization in the cytoplasm. The methionine at position 31, the phenylalanine at position 35, and the leucines at positions 38 and 40 of the NES2 sequence are required for this cytoplasmic localization. The RevM10 mutant acts as a negative control. HeLa cells were transfected with the two tandem EGFP-tagged NES2 wild type and its mutants, and the subcellular distribution of the proteins was determined after 24 h via confocal microscopy. (D) HeLa cells were transfected with EGFP-NEP or its point mutants, and the subcellular distribution of the proteins was determined after 24 h via confocal microscopy.

sion to further investigate the effect of NES2 motif on cellular localization of NEP. HeLa cells were subsequently transfected with these plasmids. Subcellular localization of these EGFP-tagged mutations was then detected by fluorescence microscopy 24 h posttransfection. Figure 4D shows that all of the mutant NEPs tested exhibit increased distribution in the cytoplasm compared with the wild-type NEP.

Roles of NES1 and NES2 in the interaction between NEP and hCRM1. Using a mammalian two-hybrid assay, Neumann et al. found that the interaction between NEP and hCRM1 is independent of NEP NES1 (26). To further elucidate the roles of these two NESs in the interaction between NEP and hCRM1, the interactions of A/chicken/Helan/12/2004 (H5N1) virus NEP or its NES-deleted mutants with hCRM1 protein in the mammalian two-hybrid system were investigated. A series of plasmids expressing NES-deleted mutants was constructed (Fig. 5A). First, the expression levels of NEP or its mutants were analyzed by immunoblot assay. Figure 5C shows that all of the constructs were expressed in 293T cells in a manner largely in line with their expected molecular weights. Next, 293T cells were cotransfected with the pBIND-NEP plasmid or its mutants, pACT-hCRM1, and the reporter plasmid pG5*luc* containing the firefly luciferase gene. Firefly luciferase activity was then measured and normalized to the *Renilla* luciferase activity 48 h posttransfection. The results illustrated that

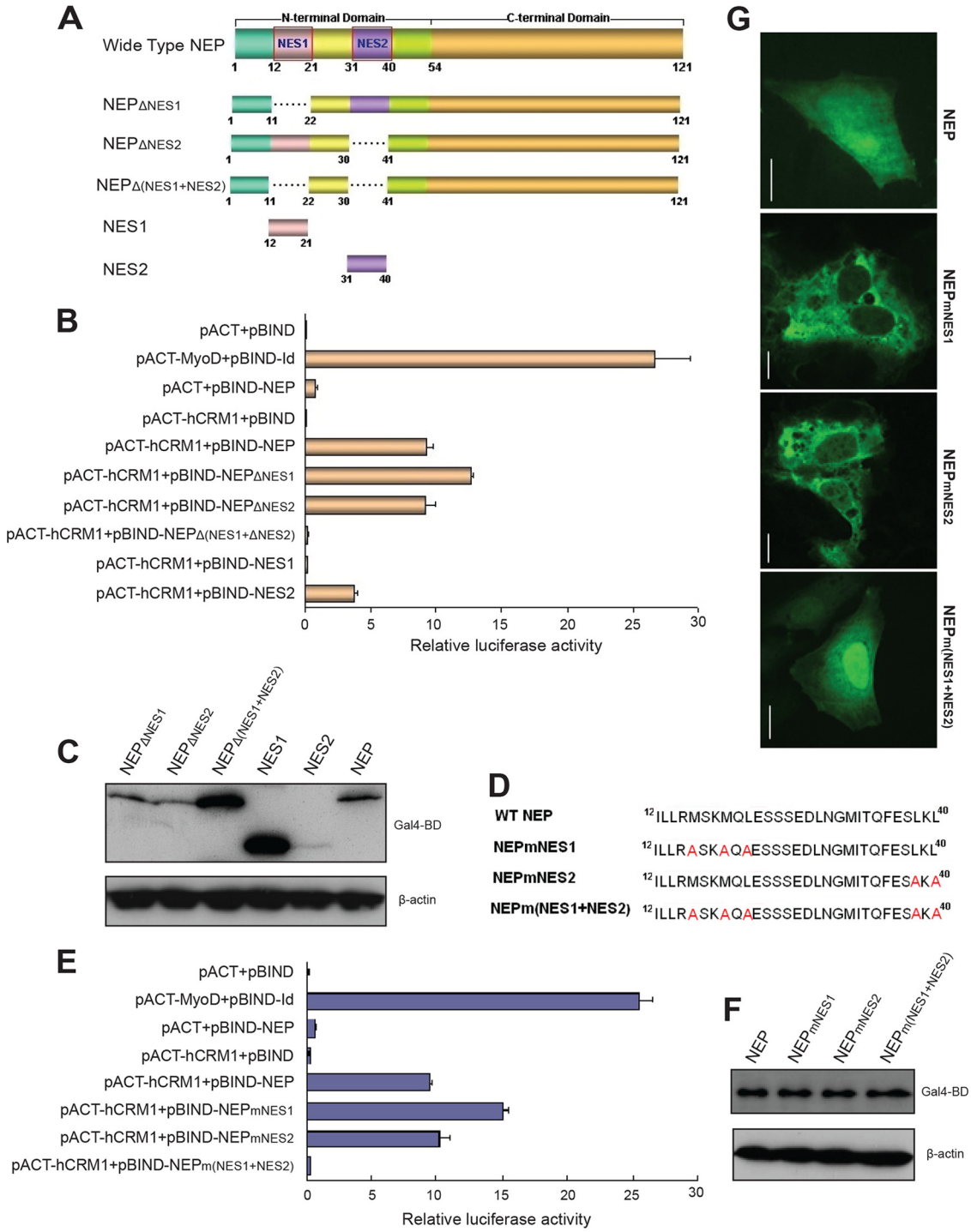

FIG 5 Characterization of the interaction between influenza virus A/chicken/Helan/12/2004 (H5N1) NEP or its mutants and the nuclear export receptor hCRM1. (A and D) Schematic representation of NEP- and NES-deleted mutants or point mutants used in the mammalian two-hybrid assays for hCRM-binding activity. (B and E) 293T cells were cotransfected with the reporter plasmid pG5*luc* and various combinations of plasmids, as indicated. About 48 h posttransfection, cell lysates were generated and luciferase activity assays were performed. The length of each bar represents the relative luciferase activity, calculated as the firefly/*Renilla* luciferase activity ratio, which reflects the binding ability between NEP or its mutants and hCRM1 in mammalian cells. pBIND-Id and pACT-MyoD (Promega) were used as positive controls. Results are shown as means ± SD for three experiments. (C and F) HEK293T cells were transfected with the pBIND-NEP or its mutants. About 48 h posttransfection, cell lysates were analyzed via Western blotting with anti-Gal4 BD polyclonal antibodies. (G) COS-7 cells were transfected with EGFP-NEP or its point mutants, and the subcellular distribution of the proteins was determined after 24 h via confocal microscopy.

TABLE 1 Amino acid sequences of mutated NEP NES2 motifs of influenza virus A/Puerto Rico/8/1934 (H1N1) used for reverse genetics manipulations

Virus type	Virus name	NES2 motif sequence[a]	Mutant virus rescued	Propagation competency[b]	Accompanying mutation(s) in NS1[c]
Wild type	R-wt	**M**ITQ**F**ES**L**K**L**	Yes		NDNTVRVSETL
Mutant	R-M1(M31I)	I*********	Yes	+++	*Y*********
	R-M2(M31A)	A*********	Yes	+++	S**********
	R-M3(F35L)	****L*****	Yes	+++	**********
	R-M4(F35A)	****A*****	Yes	+	****G******
	R-M5(F35K)	****K*****	No	ND	****E******
	R-M6(L38 M)	*******M**	Yes	+++	*******Y***
	R-M7(L38A)	*******A**	Yes	++	*******C***
	R-M8(L38R)	*******R**	No	ND	**********
	R-M9(L40F)	*********F	Yes	+++	*********I*
	R-M10(L40A)	*********A	Yes	++	*********S*
	R-M11(L38A L40A)	*******A*A	Yes	+	*******C*S*

[a] Hydrophobic residues in the conserved sites are shown in boldface. Asterisks indicate that no changes occurred in the amino acid sequences.
[b] Propagation competency compared with the wild-type virus A/Puerto Rico/8/1934 (H1N1). +++, grew at most 5-fold lower titer than wild-type virus; ++, grew at least 10-fold lower titer than the wild-type virus; +, grew over 40-fold lower titer than the wild-type virus (for more details, see Table 2). ND, not tested.
[c] Asterisks indicate that no changes occurred in the amino acid sequences.

influenza A virus NEP specifically interacted with the hCRM1 receptor, and deletion of NES1 did not abolish this interaction. In fact, a little stronger interaction between $NEP_{\Delta NES1}$ and hCRM1 was observed compared with the wild-type NEP and hCRM1 (Fig. 5B). These results are in accordance with those of a previous work (26). Furthermore, deletion of the NEP NES2 did not abolish the interaction between NEP and hCRM1, but deletion of both NEP NES1 and NEP NES2 completely abolished the NEP-hCRM1 interaction (Fig. 5B). Taken together, these results indicate that the interaction between NEP and hCRM1 is independent of either NEP NES1 or NES2. In spite of this, both the NES1 and NES2 coordinately regulate the interaction between NEP and hCRM1.

This study also determined whether or not NES1 or NES2 alone can associate with hCRM1. Two plasmids that encode the Gal4 binding domain (BD) fused to NES1 or NES2 (pBIND-NES1 or pBIND-NES2) were constructed. NES2 was able to interact with hCRM1 alone in the mammalian two-hybrid system, but NES1 showed no detectable interaction with hCRM1.

To rule out the possibility that the disrupted interactions between CRM1 and NEP deletion mutants are simply caused by the changes in conformation and stability of these NEP mutations, we further studied the interactions between NEP and CRM1 by using NEP point mutations. As shown in Fig. 5D, three NEP point mutants, named NEPmNES1, NEPmNES2, and NEPm(NES1+NES2), were constructed. The immunoblot assay indicated that the expression levels of these point mutants were similar to that of the wild-type NEP (Fig. 5F). Interactions between these NEP mutants and hCRM1 are also in accordance with those based on NEP deletion mutations (Fig. 5E). Besides these, we further investigated the distribution of NEPmNES1, NEPmNES2, and NEPm(NES1+NES2). COS-7 cells were transfected with these plasmids. Subcellular localization of expressed EGFP-tagged fusion proteins was detected using fluorescence microscopy 24 h posttransfection. As shown in Fig. 5G, the cellular distribution of the mutant proteins EGFP-NEPmNES1 and EGFP-NEPmNES2 exhibited more cytoplasmic localization than the wild-type NEP. Unlike EGFP-NEPmNES1 and EGFP-NEPmNES2, the EGFP-NEPm(NES1+NES2) mutant proteins showed increased distribution within the nucleus. These results indicated that both NES1 and NES2 contribute to the subcellular localization of NEP.

Role of NES2 in viral propagation and nuclear export of vRNPs. To further understanding of the role of the newly identified NES2 during the viral replication, we rescued recombinant viruses with mutations within the NES2 motif of the A/Puerto Rico/8/1934 (H1N1) virus NEP by using reverse genetics. Given that hydrophobic amino acid residues located on the conserved sites within NES are critical for NES functions, conserved hydrophobic residues of NES2 were substituted for with three kinds of amino acids, from one hydrophobic residue to another, to the neutral alanine, or to another phobic residue (Table 1), using site-directed mutagenesis. Based on the eight plasmid-driven reverse genetics system, nine mutant viruses from 11 mutant constructs were rescued. Sequencing of NS fragments of the mutant viruses showed the expected mutations in NEP NES2. The rescued mutant viruses have concomitant mutations at amino acid positions 188 to 198 of NS1 protein (Table 1).

The propagation properties of NEP NES2 mutant viruses were then compared with those of the wild-type A/Puerto Rico/8/1934 (H1N1) virus in MDCK cells. Briefly, MDCK cells were infected with the wild-type or mutant virus at an MOI of 0.01 and then incubated at 37°C. At 36 h postinfection, culture supernates were then collected and virus titers were determined. Based on their propagation properties, nine mutant viruses were divided into three groups (groups I, II, and III) (Table 2). Group I contained five mutant viruses, namely, R-M1(M31I), R-M2(M31A), R-M3(F35L), R-M6(L38M), and R-M9(L40F), whose titers were attenuated by less than 5-fold compared with the wild-type virus. Group II contained two mutant viruses, namely, R-M7(L38A) and R-M10(L40A), whose virus titers were reduced by about 10-fold compared with the wild-type virus. The mutant viruses in group III, namely, R-M4 (F35A) and R-M11 (L38A/L40A), were attenuated by more than 40-fold compared with the wild-type virus. The growth properties of the five mutant viruses compared with that of the wild-type virus in MDCK cells were further evaluated. MDCK cells were infected with the virus at an MOI of 0.01, and virus titers in the culture medium were determined via

TABLE 2 Propagation properties of the wild-type A/Puerto Rico/8/1934 (H1N1) virus and its NEP NES mutant viruses in MDCK cells

Virus name	Virus titer at 36 h postinfection (log_{10} $TCID_{50}$/ml)[a]	Group[b]
R-wt	8.55 ± 0.19	
R-M1(M31I)	8.35 ± 0.14	I
R-M2(M31A)	8.22 ± 0.20	I
R-M3(F35L)	8.55 ± 0.09	I
R-M4(F35A)	6.94 ± 0.20	III
R-M6(L38M)	8.00 ± 0.00	I
R-M7(L38A)	7.55 ± 0.09	II
R-M9(L40F)	8.30 ± 0.06	I
R-M10(L40A)	7.50 ± 0.17	II
R-M11(L38A L40A)	6.72 ± 0.09	III

[a] MDCK cells were infected with wild-type A/Puerto Rico/8/1934 (H1N1) virus or NEP NES2 mutant virus at an MOI of 0.01. At 36 h postinfection, the cell culture supernatants were harvested and subjected to $TCID_{50}$ assays in MDCK cells. The values shown are the means ± standard deviations from three independent determinations.
[b] Based on virus propagation properties, all mutant viruses were categorized into three groups. Group I, viruses were attenuated by less than 5-fold compared with the wild-type virus; group II, viruses were attenuated by about 10-fold compared with the wild-type virus; group III, viruses were attenuated by more than 40-fold compared with the wild-type virus.

$TCID_{50}$ tests at different times after infection. Figure 6A shows that the growth curve of the mutant virus R-M2(M31A) exhibits no significant difference compared with the wild-type virus, whereas the growth of the four other mutant viruses (groups II and III) is significantly slower than that of the wild-type virus. These data indicate that the tryptophan at position 35 and the leucines at positions 38 and 40 of NEP NES2 are functionally important for virus propagation. In order to exclude the possibility that the replication deficiency was attributed to the concomitant mutations of the A/Puerto Rico/8/1934 (H1N1) virus NS1 protein (Table 1), a series of biological functions of NS1 protein of the wild-type virus and mutant virus R-M11 were compared. First, immunoblot analysis from transfected cell lysates was performed using anti-EGFP antibody to detect the expression levels of the wild-type and mutant NS1 proteins. The data suggested that the expression level of the mutant NS1 protein is similar to that of the wild-type NS1 protein (see Fig. S1A in the supplemental material). We also determined the subcellular localization of the wild-type and mutant NS1 proteins, and the result showed that both the wild-type and mutant NS1 proteins were distributed in the cytoplasm (see Fig. S1B). This pattern of distribution was in accordance with that of NS1 protein in the previous report (35). It has been shown that influenza A virus NS1 protein can inhibit the production of alpha/beta interferon (IFN-α/β) (36–38), so we finally examined whether the mutant NS1 protein would regulate the production of IFN-α/β. The results showed that both the wild-type and mutant NS1 protein exhibited similar interferon-antagonistic properties (see Fig. S1C). Collectively, these results suggested the concomitant mutations in NS1 protein had little effect on the functions of NS1 protein. In addition, the replication deficiency of the mutant viruses is mainly attributed to the mutations of NEP NES2.

Influenza A virus NEP is crucial for vRNA synthesis and vRNP

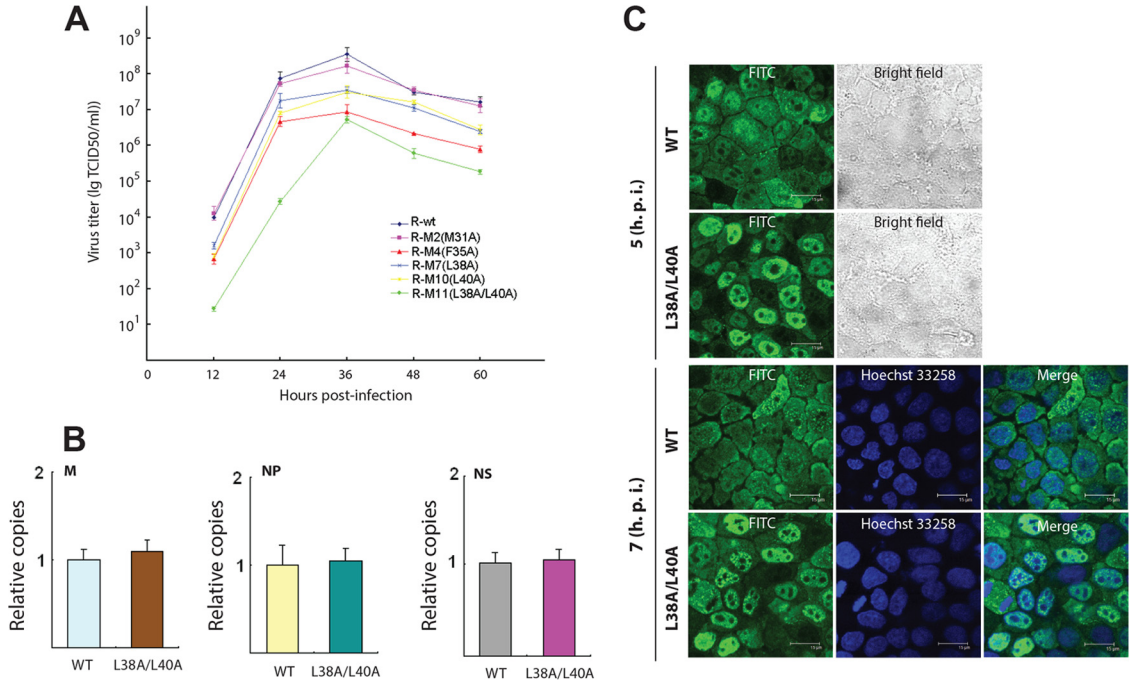

FIG 6 NEP NES2 of influenza virus A/Puerto Rico/8/1934 (H1N1) is involved in virus propagation and vRNP nuclear export. (A) Growth curves of wild-type and NEP NES2 mutant viruses in MDCK cells. MDCK cells were infected at an MOI of 0.01 with the indicated virus. About 12 to 60 h postinfection, infectious particles in the supernatant were titrated via the $TCID_{50}$ assay. Results are expressed as means ± standard deviations (SD) in triplicate. (B) MDCK cells were infected at an MOI of 1 with the wild-type or mutant R-M11(L38A L40A) virus. At 5 h postinfection (p.i.), the total RNA was isolated and real-time PCR was performed to detect vRNA copies. (C) Subcellular localization of vRNPs. MDCK cells were infected at an MOI of 1 with the wild-type (R-wt) or mutant R-M11(L38A L40A) virus. At 5 to 7 h postinfection, MDCK cells were fixed and permeabilized. vRNP localization was analyzed via immunofluorescence assay with an anti-NP antibody.

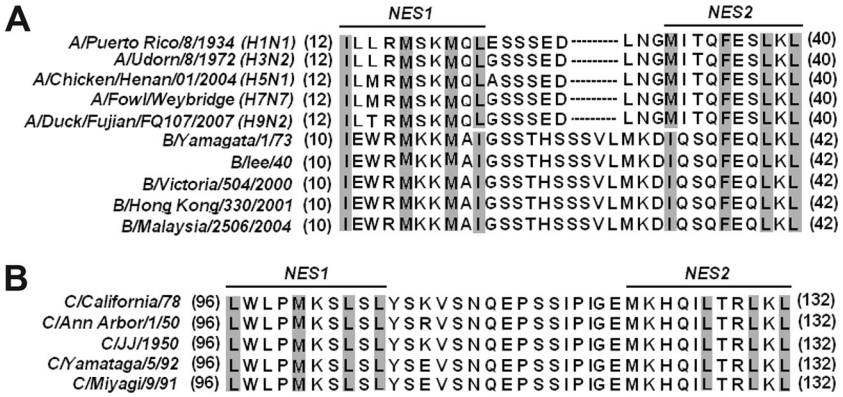

FIG 7 All influenza A, B, and C virus NEPs contain at least two conserved NES motifs. (A) Alignment of NES1 and NES2 motifs among influenza A viruses and influenza B viruses. Hydrophobic residues on the highly conserved sites are marked in gray. (B) Alignment of two NES motifs within influenza C viruses. Conserved residues are also indicated in gray.

nuclear export (11, 17, 39, 40). We sought to determine whether or not the reduced growth of the mutant viruses may be attributed to the decrease in vRNA level or restriction of vRNP nuclear export brought about by mutations introduced into the NEP NES2 sequence. First, M, NP, and NS vRNA levels of wild-type and mutant viruses were examined using real-time PCR 5 h postinfection. The result showed that there was no significant difference in vRNA levels between the wild-type and mutant viruses (Fig. 6B). Localization of vRNPs in the wild-type and mutant viruses was then observed. NP localization is a generally accepted indicator of vRNP localization (11, 18); thus, immunofluorescence assays with anti-NP antibodies were used to study the intracellular localization of vRNPs. The vRNP nuclear export abilities of the wild-type and mutant R-M11(L38A L40A) viruses were compared. MDCK cells were infected with the virus at an MOI of 1. At 5 and 7 h postinfection, the MDCK cells were fixed and examined for the intracellular localization of vRNPs. Immunofluorescence assays with anti-NP antibodies indicated an evident delay in the nuclear export of vRNPs in the mutant R-M11(L38A/L40A) virus compared with that of the wild-type virus (Fig. 6C). NEP NES2 mutation appears to impair the nuclear export of vRNPs, ultimately leading to the reduction in mutant virus growth.

The NEP NES2 motif is conserved in influenza A and B viruses. Nucleocytoplasmic transport of vRNPs is pivotal to the replication cycle of influenza A, B, and C viruses. All NEPs of influenza A, B, and C viruses possess nuclear export activity and are crucial for the nuclear export of vRNPs (11, 41). Influenza A virus NEP contains a Rev-like NES1 (amino acids 12 to 21); influenza B virus NEP also contains a Rev-like NES (amino acids 10 to 19). Paragas et al. demonstrated that influenza A virus NEP NES1 can substitute for influenza B virus NEP NES in the VLP system (41). In the present study, the second leucine-rich NES (NES2) in influenza A virus NEP was identified. NEP from influenza B virus is orthologous to that from influenza A virus; thus, we investigated whether or not influenza B virus NEP also contains a second NES. As shown in Fig. 7A, the amino acid sequences of influenza A and B virus NEPs were aligned. The results also showed that NES2 is highly conserved in both influenza A and B virus strains. Based on the sequence alignment obtained, amino acids 33 to 42 of influenza B virus NEP are postulated to be a functional NES, similar to the influenza A virus NEP NES2. Influenza C virus C/California/78 NEP has two functional NES motifs that are important for nuclear export activity (41). As shown in Fig. 7B, the two functional NES motifs are conserved in influenza C viruses. Based on these data, all influenza A, B, and C virus NEPs can be concluded to contain at least two functional NESs, and NES2 is highly conserved in influenza A and B viruses.

DISCUSSION

In the present study, a new leucine-rich nuclear export signal, NES2, was identified in influenza virus NEP. Our data show that two tandem EGFPs could be efficiently exported to the cytoplasm when fused with the NES2 motif, and identification of the NES2 motif in influenza virus NEP provides a reasonable explanation for the discrepancy obtained in previous studies. Neumann et al. (26) demonstrated that deletion of NEP NES1 does not abolish the interaction between NEP and hCRM1; in fact, such an interaction was enhanced compared with that by the full-length NEP. In our recently published study (24), we found that NEP interacts with nucleoporin 98 in an NES1-independent manner. Several leucine-rich NESs function as export adaptors by directly binding to CRM1. NEP of influenza virus has been proven to act as an adaptor protein that mediates the nuclear export of vRNPs via a CRM1-dependent pathway. Why then does the nuclear export of vRNPs exhibit a CRM1-dependent pathway, whereas NEP-CRM1 interaction follows a NES1-independent manner? Our data suggest that NEP-CRM1 interaction occurs in a NES-dependent manner and NES2 can interact with CRM1 (Fig. 5B). The $NEP_{\Delta NES1}$ mutant is localized exclusively in the cytoplasm (Fig. 1) and displays nuclear retention in the presence of LMB (Fig. 2). Thus, features of the mutant protein $NEP_{\Delta NES1}$, such as absolute cytoplasmic localization, a stronger affinity to CRM1, and striking LMB sensitivity, may be attributed to the NES2 motif.

The NES2 motif was mapped to the 31-MITQFESLKL-40 amino acid via serial deletion mutagenesis, completely matching an NES-conserved consensus (42). The NES2 motif can drive two tandem EGFPs into the cytoplasm, demonstrating that NES2 is a transferable and functional NES. What is the relationship between these two functional NESs? The results of a mammalian two-hybrid assay show that deletion of either NES1 or NES2 does not abolish NEP binding to CRM1. However, when both NES1 and NES2 are deleted, no interaction is detected. Thus, both the previously reported NES1 and the NES2 in the present study contributed to the interaction between NEP and hCRM1. Some proteins,

such as snurportin 1 (SNUPN) (43), carbohydrate-responsive binding protein (ChREBP) (44), and human cytomegalovirus UL84 protein (45), harbor at least two NESs. Recently, the crystal structure of SNUPN bound to CRM1 was reported (43, 46). Based on the three-dimensional (3D) structure obtained, the SNUPN NES1 motif, which has an α-helical extended structure, was found to bind to the conserved hydrophobic groove of the outer helices of CRM1. The NES2 motif of NEP is located in the predicted N2 α-helical region and can interact with hCRM1. Thus, the NES2 motif of NEP may also bind to the conserved hydrophobic groove.

Cellular localization of mutant NEPs that contain a series of point mutations within the NES2 motif exhibits increased cytoplasmic distribution compared with that of wild-type NEP. Furthermore, in the absence of NES1, EGFP-NEP$_{\Delta NES1}$ is localized exclusively in the cytoplasm. How can NES1 and NES2 affect the cellular distribution of NEP? The crystal structure of the C-terminal domain of NEP was determined (16), revealing an α-helical hairpin that can dimerize as a four-helix bundle. The crystal structure of the N-terminal domain of NEP has yet to be resolved but is predicted to contain two α-helices, namely, helices N1 and N2. The NES1 and NES2 motifs are located at the predicted helices N1 and N2, respectively. The C-terminal domain has a very rigid conformation, whereas the N-terminal domain of NEP is highly flexible and mobile (43, 47). Thus, we assume that point mutations within NES1 or NES2, as well as NEP deletion mutations, not only affect the nuclear export activity of NEP but also change the conformation of NEP. Conformational changes further affect the interaction between NESs and CRM1, eventually determining the cellular localization of NEP.

In summary, leucine-rich NES2 in the nuclear export domain of NEP of influenza A virus was reported, and its involvement in the nuclear export of vRNPs was demonstrated. The present data provide novel insights into the role of NEP in the nuclear transport of influenza virus vRNPs.

ACKNOWLEDGMENTS

We thank R. G. Webster (St. Jude Children's Research Hospital, Memphis, TN) for the pHW2000 plasmid. We also thank Maarten Fornerod (NCI, Amsterdam, Netherlands) for generous contributions of experimental materials.

This study was supported by the following research funds: the National 973 Project (2010CB530301), the National Natural Science Foundation of China (no. 81071346 and no. 31070141), and the Education Department of Hunan Province (no. 09K022).

S.H., J.C., and Z.C. designed the research and analyzed data. S.H., Q.C., and J.C. performed the experiments. H.W., Y.Y., and J.C. provided advice and critically read the manuscript. Z.C. supervised all experiments and wrote the article.

The authors declare that they have no conflicts of interest.

REFERENCES

1. **Görlich D, Kutay U.** 1999. Transport between the cell nucleus and the cytoplasm. Annu. Rev. Cell Dev. Biol. **15**:607–660.
2. **Fornerod M, Ohno M, Yoshida M, Mattaj IW.** 1997. CRM1 is an export receptor for leucine-rich nuclear export signals. Cell **90**:1051–1060.
3. **Ossareh-Nazari B, Bachelerie F, Dargemont C.** 1997. Evidence for a role of CRM1 in signal-mediated nuclear protein export. Science **278**:141–144.
4. **Stade K, Ford CS, Guthrie C, Weis K.** 1997. Exportin 1 (Crm1p) is an essential nuclear export factor. Cell **90**:1041–1050.
5. **Kudo N, Matsumori N, Taoka H, Fujiwara D, Schreiner EP, Wolff B, Yoshida M, Horinouchi S.** 1999. Leptomycin B inactivates CRM1/exportin 1 by covalent modification at a cysteine residue in the central conserved region. Proc. Natl. Acad. Sci. U. S. A. **96**:9112–9117.
6. **Kudo N, Wolff B, Sekimoto T, Schreiner EP, Yoneda Y, Yanagida M, Horinouchi S, Yoshida M.** 1998. Leptomycin B inhibition of signal-mediated nuclear export by direct binding to CRM1. Exp. Cell Res. **242**:540–547.
7. **Palese P.** 1977. The genes of influenza virus. Cell **10**:1–10.
8. **Boulo S, Akarsu H, Ruigrok RW, Baudin F.** 2007. Nuclear traffic of influenza virus proteins and ribonucleoprotein complexes. Virus Res. **124**:12–21.
9. **Cros JF, Palese P.** 2003. Trafficking of viral genomic RNA into and out of the nucleus: influenza, Thogoto and Borna disease viruses. Virus Res. **95**:3–12.
10. **Martin K, Helenius A.** 1991. Nuclear transport of influenza virus ribonucleoproteins: the viral matrix protein (M1) promotes export and inhibits import. Cell **67**:117–130.
11. **O'Neill RE, Talon J, Palese P.** 1998. The influenza virus NEP (NS2 protein) mediates the nuclear export of viral ribonucleoproteins. EMBO J. **17**:288–296.
12. **Richardson JC, Akkina RK.** 1991. NEP protein of influenza virus is found in purified virus and phosphorylated in infected cells. Arch. Virol. **116**:69–80.
13. **Ward AC, Castelli LA, Lucantoni AC, White JF, Azad AA, Macreadie IG.** 1995. Expression and analysis of the NEP protein of influenza A virus. Arch. Virol. **140**:2067–2073.
14. **Yasuda J, Nakada S, Kato A, Toyoda T, Ishihama A.** 1993. Molecular assembly of influenza virus: association of the NEP protein with virion matrix. Virology **196**:249–255.
15. **Lamb RA, Lai CJ.** 1980. Sequence of interrupted and uninterrupted mRNAs and cloned DNA coding for the two overlapping nonstructural proteins of influenza virus. Cell **21**:475–485.
16. **Akarsu H, Burmeister WP, Petosa C, Petit I, Müller CW, Ruigrok RW, Baudin F.** 2003. Crystal structure of the M1 protein-binding domain of the influenza A virus nuclear export protein (NEP/NS2). EMBO J. **22**:4646–4655.
17. **Robb NC, Smith M, Vreede FT, Fodor E.** 2009. NS2/NEP protein regulates transcription and replication of the influenza virus RNA genome. J. Gen. Virol. **90**:1398–1407.
18. **Iwatsuki-Horimoto K, Horimoto T, Fujii Y, Kawaoka Y.** 2004. Generation of influenza A virus NS2 (NEP) mutants with an altered nuclear export signal sequence. J. Virol. **78**:10149–10155.
19. **Bui M, Wills EG, Helenius A, Whittaker GR.** 2000. Role of the influenza virus M1 protein in nuclear export of viral ribonucleoproteins. J. Virol. **74**:1781–1786.
20. **Elton D, Simpson-Holley M, Archer K, Medcalf L, Hallam R, McCauley J, Digard P.** 2001. Interaction of the influenza virus nucleoprotein with the cellular CRM1-mediated nuclear export pathway. J. Virol. **75**:408–419.
21. **Chase GP, Rameix-Welti M, Zvirbliene A, Zvirblis G, Götz V, Wolff T, Naffakh N, Schwemmle M.** 2011. Influenza virus ribonucleoprotein complexes gain preferential access to cellular export machinery through chromatin targeting. PLoS Pathog. **7**:e1002187. doi:10.1371/journal.ppat.1002187.
22. **Malim MH, Böhnlein S, Hauber J, Cullen BR.** 1989. Functional dissection of the HIV-1 Rev *trans*-activator—derivation of a *trans*-dominant repressor of Rev function. Cell **58**:205–214.
23. **Ma K, Roy AM, Whittaker GR.** 2001. Nuclear export of influenza virus ribonucleoproteins: identification of an export intermediate at the nuclear periphery. Virology **282**:215–220.
24. **Chen J, Huang S, Chen Z.** 2010. Human cellular protein nucleoporin hNup98 interacts with influenza A virus NS2/nuclear export protein and overexpression of its GLFG repeat domain can inhibit virus propagation. J. Gen. Virol. **91**:2474–2484.
25. **Nayak DP, Hui EK, Barman S.** 2004. Assembly and budding of influenza virus. Virus Res. **106**:147–165.
26. **Neumann G, Hughes MT, Kawaoka Y.** 2000. Influenza A virus NS2 protein mediates vRNPs nuclear export through NES-independent interaction with hCRM1. EMBO J. **19**:6751–6758.
27. **Chen Z, Sahashi Y, Matsuo K, Asanuma H, Takahashi H, Iwasaki T, Suzuki Y, Aizawa C, Kurata T, Tamura S.** 1998. Comparison of the ability of viral protein-expressing plasmid DNAs to protect against influenza. Vaccine **16**:1544–1549.
28. **Zheng L, Wang F, Yang Z, Chen J, Chang H, Chen Z.** 2009. A single immunization with HA DNA vaccine by electroporation induces early

protection against H5N1 avian influenza virus challenge in mice. BMC Infect. Dis. **9**:17. doi:10.1186/1471-2334-9-17.
29. **Hoffmann E, Neumann G, Kawaoka Y, Hobom G, Webster RG.** 2000. A DNA transfection system for generation of influenza A virus from eight plasmids. Proc. Natl. Acad. Sci. U. S. A. **97**:6108–6113.
30. **Huang S, Chen J, Wang H, Sun B, Wang H, Zhang Z, Zhang X, Chen Z.** 2009. Influenza A virus matrix protein 1 interacts with hTFIIIC102-s, a short isoform of the polypeptide 3 subunit of human general transcription factor IIIC. Arch. Virol. **154**:1101–1110.
31. **Hoffmann E, Stech J, Guan Y, Webster RG, Perez DR.** 2001. Universal primer set for the full-length amplification of all influenza A viruses. Arch. Virol. **146**:2275–2289.
32. **Ge Q, McManus MT, Nguyen T, Shen CH, Sharp PA, Eisen HN, Chen J.** 2003. RNA interference of influenza virus production by directly targeting mRNA for degradation and indirectly inhibiting all viral RNA transcription. Proc. Natl. Acad. Sci. U. S. A. **100**:2718–2723.
33. **Reed LJ, Muench H.** 1938. A simple method of estimating fifty percent endpoints. Am. J. Hyg. (Lond.) **27**:493–497.
34. **Watanabe K, Takizawa N, Katoh M, Hoshida K, Kobayashi N, Nagata K.** 2001. Inhibition of nuclear export of ribonucleoprotein complexes of influenza virus by leptomycin B. Virus Res. **77**:31–42.
35. **Han H, Cui Z, Wang W, Zhang Z, Wei H, Zhou Y, Zhang X.** 2010. New regulatory mechanisms for the intracellular localization and trafficking of influenza A virus NS1 protein revealed by comparative analysis of A/PR/8/34 and A/Sydney/5/97. J. Gen. Virol. **91**:2907–2917.
36. **Mibayashi M, Martínez-Sobrido L, Loo YM, Cárdenas WB, Gale M, Jr, GarcíA-Sastre A.** 2007. Inhibition of retinoic acid-inducible gene I-mediated induction of beta interferon by the NS1 protein of influenza A virus. J. Virol. **81**:514–524.
37. **Opitz B, Rejaibi A, Dauber B, Eckhard J, Vinzing M, Schmeck B, Hippenstiel S, Suttorp N, Wolff T.** 2007. IFNbeta induction by influenza A virus is mediated by RIG-I which is regulated by the viral NS1 protein. Cell. Microbiol. **9**:930–938.
38. **Wang X, Li M, Zheng H, Muster T, Palese P, Beg A, GarcíA-Sastre A.** 2000. Influenza A virus NS1 protein prevents activation of NF-kappaB and induction of alpha/beta interferon. J. Virol. **74**:11566–11573.
39. **Bullido R, Gómez-Puertas P, Saiz MJ, Portela A.** 2001. Influenza A virus NEP (NS2 protein) downregulates RNA synthesis of model template RNAs. J. Virol. **75**:4912–4917.
40. **Perez J, Varble A, Sachidanandam R, Zlatev I, Manoharan M, GarcíA-Sastre A, tenOever BR.** 2010. Influenza A virus-generated small RNAs regulate the switch from transcription to replication. Proc. Natl. Acad. Sci. U. S. A. **107**:11525–11530.
41. **Paragas J, Talon J, O'Neill RE, Anderson DK, GarcíA-Sastre A, Palese P.** 2001. Influenza B and C virus NEP (NS2) proteins possess nuclear export activities. J. Virol. **75**:7375–7383.
42. **la Cour T, Gupta R, Rapacki K, Skriver K, Poulsen FM, Brunak S.** 2003. NESbase version 1.0: a database of nuclear export signals. Nucleic Acids Res. **31**:393–396.
43. **Dong X, Biswas A, Süel KE, Jackson LK, Martinez R, Gu H, Chook YM.** 2009. Structural basis for leucine-rich nuclear export signal recognition by CRM1. Nature **458**:1136–1141.
44. **Fukasawa M, Ge Q, Wynn RM, Ishii S, Uyeda K.** 2010. Coordinate regulation/localization of the carbohydrate responsive binding protein (ChREBP) by two nuclear export signal sites: discovery of a new leucine-rich nuclear export signal site. Biochem. Biophys. Res. Commun. **391**:1166–1169.
45. **Lischka P, Rauh C, Mueller R, Stamminger T.** 2006. Human cytomegalovirus UL84 protein contains two nuclear export signals and shuttles between the nucleus and the cytoplasm. J. Virol. **80**:10274–10280.
46. **Monecke T, Güttler T, Neumann P, Dickmanns A, Görlich D, Ficner R.** 2009. Crystal structure of the nuclear export receptor CRM1 in complex with Snurportin1 and RanGTP. Science **324**:1087–1091.
47. **Lommer BS, Luo M.** 2002. Structural plasticity in influenza virus protein NS2 (NEP). J. Biol. Chem. **277**:7108–7117.